SEY AND OTHER MATERIAL PROPERTIES STUDIED AT CRYOGENIC TEMPERATURES

L.Spallino*, M. Angelucci, R. Larciprete[1] and R. Cimino, LNF-INFN, Frascati (Roma), Italy.
[1]also at CNR-ISC Istituto dei Sistemi Complessi, Roma, Italy.

Abstract

A very low secondary electron yield is confirmed to be the fingerprint of laser treated copper substrates. In future high energy particle accelerators, this feature offers unquestionable advantages for electron cloud mitigation purposes. Thermal programmed desorption between 20 and 70 K by dosing Ar multilayers of different thicknesses on a laser treated copper substrate and on its flat counterpart are here reported. The results show that, as a consequence of their nanostructured porous morphology, the desorption of gas from the laser treated substrates occurs in a much broader and higher temperature range with respect to what is observed from the flat substrates. These findings suggest that vacuum transient effects against temperature fluctuations should be better evaluated, if such surfaces would be included as cryogenic vacuum components in accelerators.

INTRODUCTION

The secondary emission yield (SEY) is an intrinsic property of materials, accounting for the capability to produce secondary electrons when an electron impacts the surface. From plasma physics to satellite and radio-frequency applications, SEY determination is therefore of paramount importance. SEY could play a fundamental role in governing, for example, space-charge effects and/or radio-frequency break down [1–3]. In the same way, SEY is a crucial parameter for all modern high-energy positively charged particle accelerators for which, as a consequence of the strong coupling between the charged particle beam and the cloud of low energy electrons, electron-cloud effects (ECE) may cause machine and beam instabilities [4–10]. Efficient ECE mitigation strategies are nowadays considered as a priority for the commissioning of the High Luminosity-Large Hadron Collider (HL-LHC) [19,20] and for the proton-proton Future Circular Collider (FCC-hh) [21]. These strategies have the objective to reduce SEY [8, 11–14]. Surface geometrical modifications have been proved to be quite effective [1–3, 12, 15, 16] and recently an engineering method based on laser ablation (LASE) has been proposed to this purpose. LASE can modify the surface at the nanoscale. It ensures an impressive reduction of SEY down to values even less then 1, depending on the detailed process and substrate material [18, 38]. The advantageous results of laser processing have brought laser treated copper (LASE-Cu) surfaces to be proposed to be used in future accelerator technology. LASE-Cu is a potential candidate to mitigate ECE expected to occur on the beam screen (BS) in the cold bore of the dipoles of HL-LHC [19, 20] and FCC-hh [21]. However, before definitely including LASE-surfaces in the machine design, the consequences of having a rough rather than a flat wall in the cryogenic ultra high vacuum (UHV) should be carefully evaluated.

At cryogenic temperature, even small and unavoidable temperature (T) fluctuations of the accelerator vacuum components may cause undesirable vacuum transient. If T is low enough, residual gas molecules like H_2, CO, CO_2, H_2O, CH_4, etc. may be adsorbed on the cryogenic walls. Any T increase may induce their desorption and an unwanted pressure increase. [22]. High p, even if only for a short time or in a small section of the accelerator, may indeed have significant detrimental effects on machine performances. Therefore, a cryogenic vacuum system should avoid vacuum transient and pressure excursions [23, 24]. For this reason, the BS in the cold bore of LHC is efficiently working at T~20 K. Whereas, for costs reasons and available cooling budget, the cold bore of FCC-hh has been proposed to operate in a temperature range between 40 K and 60 K [25]. At these temperatures, indeed, the saturated vapor pressure curves of the residual gas species adsorbed on the BS flat surfaces [26] are compatible with the operational pressure range planned for these machines [27]. This could not be the case for strongly *modified* surfaces. In the case of any porous structure and, specifically, for laser treated samples, the nanostructure surface may trap more efficiently adatoms even in presence of adsorbed contaminants. Shifts of the desorption T at higher values in respect to the one foreseen by the saturated vapor pressure curve and a significant spread of the desorption T have been already observed in various porous systems [28–31]. Therefore, in case of strongly morphologically *modified* surfaces in the cryogenic vacuum system, the evaluation of the saturated vapor pressure curves may not be sufficient to assess the absence of vacuum transient during small temperature fluctuations. The investigation of the behavior of adsorbates on the artificially roughed surfaces as a function of temperature is then mandatory.

Here, the SEY characteristic of the LASE-Cu sample is presented, confirming the unquestionable advantages offered by such substrates as ECE mitigators. In accordance with our previous work [32], the thermal desorption characteristics of Ar dosed on the LASE-Cu are also reported and compared to the ones coming from the flat counterpart. These results, intimately connected with the nanostructured porous morphology of the LASE-Cu materials, show possible troubling consequences that could arise by exploiting them as cryogenic vacuum components of accelerators.

* luisa.spallino@lnf.infn.it

EXPERIMENTAL

Experiments were performed at the Material Science Laboratory of the LNF-INFN (Frascati, Italy), in a μ-metal UHV chamber, having base pressure $p<1\cdot10^{-10}$ mbar and equipped with a close cycle He cooled cryogenic manipulator at the end of which the sample holder is mounted. The temperature of the samples can be increased in the range 15-400 K by a resistive heater controlled by a diode with a 0.2 K precision. The sample is electrically insulated, therefore sample drain current can be measured and, with it, Secondary Electron Yield. SEY is the ratio of the number of electrons leaving the sample surface (I_{out}) to the number of incident electrons (I_p) per unit area. Experimental details are reported elsewhere [5, 8, 32–35]. SEY was determined by measuring I_p and the total sample current I_s. Since I_{out}= I_p-I_s, then:

$$SEY = \frac{I_{out}}{I_p} = 1 - \frac{I_s}{I_p} \quad (1)$$

I_p is measured by means of a Faraday cup positively biased in order to prevent back-scattered re-emission to vacuum, whereas a negative bias voltage of V_s=-75 V is applied to the sample to determine I_s. SEY is measured as a function of the primary electron energy coming from an Omicron electron gun using a standard LaB_6 cathode. The electron beam was set to be smaller than 0,5 mm^2 in transverse cross-sectional area at the sample surface. The SEY measurements were performed at normal incidence, by using electron beam currents of a few nA to induce minimal electron-desorption during data acquisition.

Desorption was studied as a function of T, performing Thermal Programmed Desorption (TPD) measurements by using a quadrupole mass spectrometer (Hiden, HAL 3F PIC) while heating the sample with a rate of 0.005 K/s. Gas was delivered on the substrate held at 15-18 K through a specially designed gas-dosing system. This system has chicanes to reduce the speed of the impinging particles and it ends up with an 8×8 mm^2 dosing square, which nearly exactly matches the sample size. The doser can be inserted very close (< than 1 mm) to the sample surface or retracted away from it. The first configuration allows to reduce the gas adsorbed on the cold manipulator and then the background signal in the TPD measurements. In the retracted position the amount of gas seen by the sample is the same as the one measured by the pressure gauge and mass spectrometer, therefore a dose calibration can be performed. The gas was dosed through a leak valve at a pressure $p\sim1.2\cdot10^{-9}$ mbar. The dosing unit are given in Langumir (1L=$1.33\cdot10^{-6}$ mbar·s). A 1 L dose (performed with the retracted doser) on the *flat* polycrystalline surface can be approximately assumed to be 1 monolayer (ML), where 1 ML≈10^{15} atoms/cm^2. This conversion is obtained by considering a mean density of Cu atoms on a polycrystalline surfaces lacking crystalline order and assuming an Ar sticking coefficient close to 1 [36]. This equivalence has been used when calibrating the coverage on the *flat* sample by using SEY. LASE-Cu has an actual surface available for sticking Ar significantly larger than its sample geometrical surface. Therefore, the thickness of an Ar layer could be different on the porous and on the *flat* substrates even for nominally equal doses. Moreover, the assumption that the Ar pressure seen by the *flat* surface is homogeneous in all the porous fractals of the LASE-Cu cannot be considered to be valid. Therefore, the number of atoms deposited onto the LASE-Cu may depend on the actual sample nanostructure and coverages in ML on LASE-Cu results ill-defined. Since the task is to compare the behavior of LASE and *flat* Cu, we use Langmuir unit as common variable for both cases.

Two categories of Cu sample were considered for the present investigation: a *flat* Cu substrate and a representative sample of the LASE-Cu materials. The *flat* substrate is a polycrystalline Cu (poly-Cu) and was investigated both as received and Ar^+ sputtered at 1 keV with a current of ~15 μA measured on the sample at a pressure of p_{Ar}=8×10^{-6} mbar. These sputtering parameters are consistent with a cleaning procedure which does not increase the pristine roughness of the surface [37]. The Ar multilayer TPD results coming from it is anyway independent of the surface cleanliness. The LASE-Cu consists in copper colaminated stainless steel. Its surface is engineered by pulsed laser ablation [38] and its morphology was probed by Scanning Electron Microscopy (SEM) using a SNE-3200M Tabletop SEM.

RESULTS AND DISCUSSION

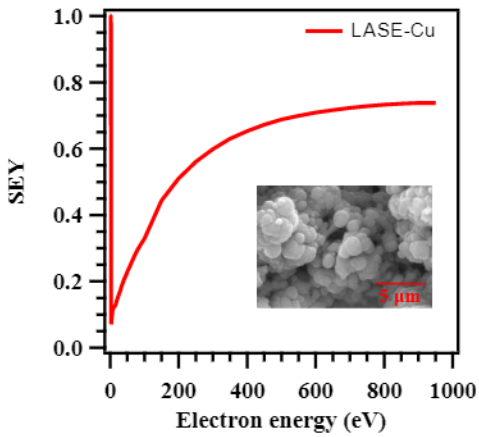

Figure 1: SEY curve at room temperature of the LASE-Cu sample under investigation. A SEM micrograph of the sample is reported in the inset.

Figure 1 shows a typical secondary emission curve acquired at room temperature from the LASE-Cu sample under investigation. In accordance with literature [38], it is characterized by an impressive low SEY (≈0.74 at 900 eV) determined by the peculiar morphological features represented by the SEM micrograph shown in the inset. It is worth to note that the low energy region of the SEY curve is measured in the LASE-Cu sample by us for the first time. A clear decrease towards SEY≈0.1 is observed for impinging electron energies close to 0 eV, as in the case of clean metallic

surfaces [35, 37]. The submicrometric highly porous network acts as a trap both for the incoming primary electrons and for secondary electrons. This qualifies such class of materials as ECE mitigators. When held at cryogenic temperature, the SEY properties of the LASE-Cu sample do not significantly change in the energy range over ~100 eV, while small SEY variations are observed in the low energy region (curve not reported). It is known, indeed, that keeping the sample at low temperature for some time determines the progressive adsorption of residual gas molecules (mainly H_2O, CO, CO_2 and CH4) [37], slightly modifiyng the low energy SEY region.

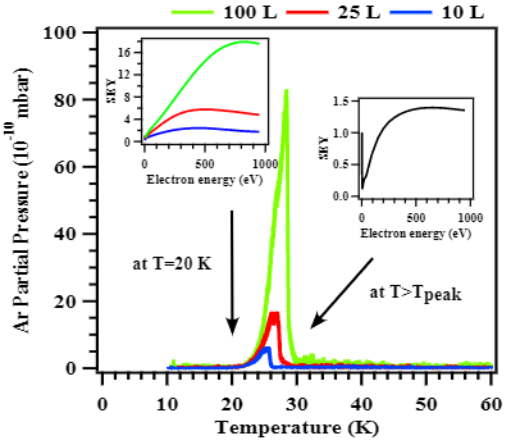

Figure 2: TPD from poly-Cu after dosing 10, 25 100 L of Ar. The SEY curves related to the given doses are reported in the inset, below (left) and after (right) the desorption peak.

To evaluate the vacuum behavior of LASE-Cu against temperature fluctuations by TPD, a preliminary study has been carried out on the poly-Cu sample to be used as reference system and to properly set the parameters for all the TPD measurements. Three increasing Ar doses were considered, namely 10, 25 and 100 L. Such high doses on the flat sample correspond to have multilayers on the substrate. This is the coverage typically expected to occur in long exposures to residual gasses in an accelerator cryogenic environment [23].

In Fig. 2 the Ar TPD results from the poly-Cu sample are shown. The curves show a sharp peak at T~28-30 K, having a Full Width at Half Maximum FWHM~4 K. The TPD area linearly increases with the Ar dose. This single peak corresponds to the desorption of a condensed thick Ar layer, as evidenced by the SEY curves acquired for each coverage below (left panel) and above (right panel) the relative desorption peak. Indeed, at T=20 K (below the desorption peaks), SEY characteristics depend on the actual Ar thickness, in good agreement with literature results [39]. Just above each desorption peak (right panel), the SEY curve is the one of the bare poly-Cu substrate for all cases, thus indicating the transition temperatures at which the gas multilayer desorbs from the surface [26, 40].

It is worth to note how sensitive is SEY to variations in Ar coverages, showing the effectiveness of using this simple spectroscopy as a technique capable to estimate them. By doing so, we can precisely (±10%) estimate the effective dose seen by the samples when dosing close to its surface even if, in this latter case, the pressure measured by the gauge and quadrupole is not representative of the Ar pressure seen by the surface. Moreover, the remarkable sensitivity of SEY to the presence of any overlayer allows also to calibrate the temperature read on the manipulator diode against the real surface temperature and to address the transition temperatures at which the gas multilayer desorbs to the multilayer desorption temperature as foreseen by literature.

The TPD data shown in Fig. 2 for the flat poly-Cu are in agreement with previous literature findings [41–43]. This single peak corresponds to the desorption of a condensed thick Ar layer. Its temperature is determined by the weak Ar-Ar Van der Waals interaction energies [26, 40]. Above this peak, a ~10, 25, 100 times smaller signal is expected to appear due to the desorption of the first monolayer [42, 43]. At present, our set-up does not allow to observe it since not only it is too small, but probably hidden below the manipulator background signal which has been set to zero. However, at this stage, the investigation of the monolayer/submonolayer regime is out of the scope of the present work.

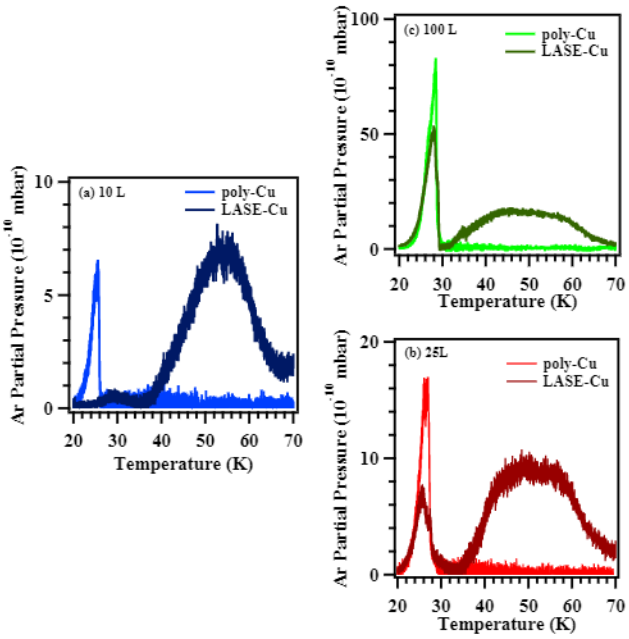

Figure 3: TPD curves obtained monitoring the desorption of 10 L (a), 25 L (b), and 100 L (c) of Ar dosed on the LASE-Cu sample (dark color lines) and on flat Cu substrate (light color lines).

The desorption curves measured on the Ar dosed LASE-Cu surface are reported in Fig. 3). For the sake of comparison the TPD profiles obtained from the flat counterpart at equal Ar doses are reported in each panel. The Ar TPD curves from LASE-Cu are characterized by broad profiles, whose peak temperatures and widths depend on the Ar dose. On increasing the Ar coverage by dosing 10 (a), 25 (b) and 100 L (c), the almost bell-shaped curves are centered at T~56 K, T~52 K and T~50 K, and have FWHM of about 15, 20

and 25 K, respectively. Moreover, after 25 and 100 L, the Ar desorption at T~28-30 K is also observed.

The Ar desorption behavior from the LASE surfaces indicates a significant dependence of the process on the surface morphology. On one hand, micro and nano-structuring dramatically increases the specific surface, making the area accessible to atomic/molecular species much larger than the one available in the flat sample. On the other hand, such a nanostructured morphology determines a local increase of the adsorption energy for the Ar atoms in correspondence of under-coordinated sites and defects [44–46]. The desorption of the Ar atoms close to defected surfaces and/or trapped in the pores of the LASE-Cu surface is shifted to higher temperature. The progressive occupation of all available adsorption sites (pores wall included) could then explain the gradual broadening of the TPD peak above 30 K observed for the LASE-Cu with increasing Ar dose. On the contrary, multilayer Ar atoms which basically feel only the Ar-Ar forces, desorb around 28-30 K, as in the case of the flat sample.

Those results are better discussed in [32]. Similar results were observed by dosing the two different Cu surfaces with gasses typically expected to be part of the residual gas composition of any accelerator vacuum system (H_2, CO and CH_4) [32, 47]. This confirms the validity of using Ar as a paradigmatic system to investigate the vacuum behaviour of the porous surfaces.

CONCLUSION

In summary, the intrinsic morphological structure confers to the LASE-Cu samples a very low SEY (SEY<1 in the energy range 0-1000 eV), both at room and cryogenic temperature. This makes such a class of materials optimal e^--cloud suppressors and, then, promising components of the future high energy particle accelerators. On the other hand, Ar TPD measurements from LASE-Cu sample have evidenced that, as a consequence of the nanostructured porous morphology, the gas desorption occurs at a higher than expected temperature and spreads over a broad range. Therefore, their vacuum behaviour at cryogenic conditions against temperature fluctuation could give rise to troubling consequences on the usually very stringent vacuum requirements of most cryogenic accelerators. In conclusion, while the use and optimization of LASE surfaces to mitigate SEY is quite advanced, a significant additional experimental campaign is necessary to validate their use in future accelerators. In particular, since non-thermal desorption processes are acknowledged to markedly contribute to accelerator vacuum behavior, photo and electron induced desorption yield should also be carefully studied.

ACKNOWLEDGEMENTS

This work was supported by The European Circular Energy- Frontier Collider Study (EuroCirCol) project (Grant No. 654305) and by the MICA project funded by INFN Scientific National Committee 5. We thank V. Baglin, P. Chiggiato, R. Kersevan, O. Malyshev, and R. Valizadeh for useful discussions and for the LASE samples. The DAΦNE-L team is acknowledged for technical assistance.

REFERENCES

[1] C. Swanson and I. D. Kaganovich, J. Appl. Phys. 120, 213302 (2016)

[2] C. Swanson and I. D. Kaganovich, J. Appl. Phys. 122, 043301 (2017)

[3] V. Nistor, L. A. Gonzalez, L. Aguilera, I. Montero, L. Galan, U. Wochner, and D. Raboso, Appl. Surf. Sci. 315, 445 (2014)

[4] G. Rumolo, A. Z. Ghalam, T. Katsouleas, C. K. Huang, V. K. Decyk, C. Ren, W. B. Mori, F. Zimmermann, and F. Ruggiero, Phys. Rev. Spec. Top. Accel. Beams 6, 081002 (2003)

[5] R. Cimino, I. Collins, M. Furman, M. Pivi, F. Ruggiero, G. Rumolo and F. Zimmermann, Phys. Rev. Lett. 93, 014801 (2004)

[6] F. Zimmermann, Phys. Rev. Spec. Top. Accel. Beams 7, 124801 (2004)

[7] ECLOUD'12: Joint INFN-CERN-EuCARD-AccNet Workshop on Electron-Cloud Effects, CERN Yellow Reports: Conference Proceedings, edited by R. Cimino, G. Rumolo, and F. Zimmermann (CERN, Geneva, 2013)

[8] R. Cimino and T. Demma, Int. J. Mod. Phys. A 29, 1430023 (2014)

[9] G. Rumolo and G. Iadarola, in CERN Yellow Reports: School Proceedings (2017), Vol. 3, p. 411

[10] K. Ohmi, F. Zimmermann, L. Mether, and D. Schulte, "Study of electron cloud instabilities in fcc-hh," Technical Report CERN-ACC-2015-285 (2015)

[11] Y. Suetsugu, K. Kanazawa, K. Shibata, and H. Hisamatsu, Nucl. Instrum. Methods Phys. Res., A 556, 399 (2006)

[12] M. Pivi, F. King, R. Kirby, T. Raubenheimer, G. Stupakov, and F. Le Pimpec, J. Appl. Phys. 104, 104904 (2008)

[13] Y. Suetsugu, H. Fukuma, L. Wang, M. Pivi, A. Morishige, Y. Suzuki, M. Tsukamoto, and M. Tsuchiya, Nucl. Instrum. Methods Phys. Res., A 598, 372 (2009)

[14] C. Yin Vallgren, G. Arduini, J. Bauche, S. Calatroni, P. Chiggiato, K. Cornelis, P. C. Pinto, B. Henrist, E. Metral, H. Neupert, G. Rumolo, E. Shaposhnikova, and M. Taborelli, Phys. Rev. Spec. Top. Accel. Beams 14, 071001 (2011)

[15] A. Krasnov, Vacuum 73, 195 (2004)

[16] M. Ye, D. Wang, and Y. He, J. Appl. Phys. 121, 124901 (2017)

[17] R. Valizadeh, O. B. Malyshev, S. Wang, S. A. Zolotovskaya, W. Allan Gillespie, and A. Abdolvand, Appl. Phys. Lett. 105, 231605 (2014)

[18] R. Valizadeh, O. Malyshev, S. Wang, T. Sian, M. D. Cropper, and N. Sykes, Appl. Surf. Sci. 404, 370 (2017)

[19] See http://hilumilhc.web.cern.ch/ for for details on the project

[20] G. Apollinari, I. B. Alonso, O. Br€uning, P. Fessia, M. Lamont, L. Rossi, and L. Tavian, High-Luminosity Large Hadron Collider (HL-LHC): Technical Design Report (CERN, 2017)

[21] See http://fcc.web.cern.ch/ for details on the project

[22] C. Benvenuti, J. Cazeneuve, P. Chiggiato, F. Cicoira, A. E. Santana, V. Johanek, V. Ruzinov, and J. Fraxedas, Vacuum 53, 219 (1999)

[23] V. Baglin, "Vacuum transients during LHC operation," in 1st LHC Project Workshop, Chamonix, France, 19–23 January (2004), p. 275

[24] W. C. Turner, J. Vac. Sci. Technol., A 14, 2026 (1996)

[25] F. J. P. Rodriguez, P. Chiggiato, C. Garion, J. F. Topham, and on behalf of EuroCirCol WP4, "Preliminary beam screen and beam pipe engineering design: Deliverable D4.3," Technical Report No. CERN-ACC-2019-0023 (CERN, Geneva, 2017)

[26] R. E. Honig and H. O. Hook, RCA Rev. 21, 360 (1960)

[27] V. Baglin, L. Tavian, P. Lebrun, and R. van Weelderen, "Cryogenic beam screens for high-energy particle accelerators," Technical Report CERN-ATS- 2013-006 (2013)

[28] J. Thrower, M. Collings, F. Rutten, and M. McCoustra, Mon. Not. R. Astron. Soc. 394, 1510 (2009)

[29] A. Paldor, G. Toker, Y. Lilach, and M. Asscher, Phys. Chem. Chem. Phys. 12, 6774 (2010)

[30] A. Clemens, L. Hellberg, H. Gr€onbeck, and D. Chakarov, Phys. Chem. Chem. Phys. 15, 20456 (2013)

[31] T. Suhasaria, J. Thrower, and H. Zacharias, Mon. Not. R. Astron. Soc. 472, 389–399 (2017)

[32] L. Spallino, M. Angelucci, R. Larciprete and R. Cimino, Appl. Phys. Lett. 114, 153103 (2019)

[33] R. Cimino, M. Commisso, D. R. Grosso, T. Demma, V. Baglin, R. Flammini and R. Larciprete, Phys. Rev. Lett. 109, 064801 (2012)

[34] R. Larciprete, D. R. Grosso, M. Commisso, R. Flammini and R. Cimino, Phys. Rev. Spec. Top. Accel. Beams 16, 011002 (2013)

[35] R. Cimino, L. A. Gonzalez, R. Larciprete, A. Di Gaspare, G. Iadarola, and G. Rumolo, Phys. Rev. Spec. Top. Accel. Beams, 18, 051002 (2015)

[36] L. L. Levenson, J. Vac. Sci. Technol. 8, 629 (1971)

[37] L. Gonzalez, M. Angelucci, R. Larciprete, and R. Cimino, AIP Adv. 7, 115203 (2017)

[38] R. Valizadeh, O. B. Malyshev, S. Wang, S. A. Zolotovskaya, W. Allan Gillespie and A. Abdolvand, Appl. Phys. Lett. 105, 231605 (2014)

[39] J. Cazaux, Y. Bozhko, and N. Hilleret, Phys. Rev. B 71, 035419 (2005)

[40] A. Ferreira and L. Lobo, J. Chem. Thermodyn. 40, 1621 (2008)

[41] M. Stichler, P. Zebisch, M. Weinelt, and H.-P. Steinr€uck, Surf. Sci. 348, 370 (1996)

[42] W. Berthold, P. Feulner, and U. H€ofer, Chem. Phys. Lett. 358, 502 (2002)

[43] A. Damm, K. Schubert, J. G€udde, and U. H€ofer, Phys. Rev. B 80, 205425 (2009)

[44] J.Y. Park, S.J. Kahng, U. Ham, Y. Kuk, K. Miyake, K. Hata, and H. Shigekawa, Phys. Rev. B 60, 16934 (1999)

[45] P. Ayotte, R. S. Smith, K. P. Stevenson, Z. Dohnalek, G. A. Kimmel, and B. D. Kay, J. Geophys. Res. Planets 106, 33387 (2001)

[46] L. Baker, B. Holsclaw, A. E. Baber, H. L. Tierney, E. C. H. Sykes, and A. J. Gellman, J. Phys. Chem. C 114, 18566 (2010)

[47] L. Spallino, M. Angelucci, R. Larciprete and R. Cimino, article in preparation.